The retromer is co-opted to deliver lipid enzymes for the biogenesis of lipid-enriched tombusviral replication organelles

Zhike Feng[a], Jun-ichi Inaba[a], and Peter D. Nagy[a,1]

[a]Department of Plant Pathology, University of Kentucky, Lexington, KY 40546

Edited by George E. Bruening, University of California, Davis, CA, and approved November 5, 2020 (received for review July 29, 2020)

Biogenesis of viral replication organelles (VROs) is critical for replication of positive-strand RNA viruses. In this work, we demonstrate that tomato bushy stunt virus (TBSV) and the closely related carnation Italian ringspot virus (CIRV) hijack the retromer to facilitate building VROs in the surrogate host yeast and in plants. Depletion of retromer proteins, which are needed for biogenesis of endosomal tubular transport carriers, strongly inhibits the peroxisome-associated TBSV and the mitochondria-associated CIRV replication in yeast and *in planta*. In vitro reconstitution revealed the need for the retromer for the full activity of the viral replicase. The viral p33 replication protein interacts with the retromer complex, including Vps26, Vps29, and Vps35. We demonstrate that TBSV p33-driven retargeting of the retromer into VROs results in delivery of critical retromer cargoes, such as 1) Psd2 phosphatidylserine decarboxylase, 2) Vps34 phosphatidylinositol 3-kinase (PI3K), and 3) phosphatidylinositol 4-kinase (PI4Kα-like). The recruitment of these cellular enzymes by the co-opted retromer is critical for de novo production and enrichment of phosphatidylethanolamine phospholipid, phosphatidylinositol-3-phosphate [PI(3)P], and phosphatidylinositol-4-phosphate [PI(4)P] phosphoinositides within the VROs. Co-opting cellular enzymes required for lipid biosynthesis and lipid modifications suggest that tombusviruses could create an optimized lipid/membrane microenvironment for efficient VRO assembly and protection of the viral RNAs during virus replication. We propose that compartmentalization of these lipid enzymes within VROs helps tombusviruses replicate in an efficient milieu. In summary, tombusviruses target a major crossroad in the secretory and recycling pathways via coopting the retromer complex and the tubular endosomal network to build VROs in infected cells.

virus–host interaction | virus replication | retromer complex | viral replication organelle | lipid biosynthesis

Viruses are intracellular parasites which co-opt cellular resources to produce abundant viral progeny. Positive-strand (+)RNA viruses replicate on subcellular membranes by forming viral replication organelles (VROs) (1–5). VROs sequester the viral proteins and viral RNAs together with co-opted host factors to provide an optimal subcellular environment for the assembly of numerous viral replicase complexes (VRCs), which are then responsible for robust viral RNA replication. VROs also spatially and temporally organize viral replication. Importantly, the VROs hide the viral RNAs from cellular defense mechanisms as well (5, 6). VROs consist of extensively remodeled membranes with unique lipid composition. How viruses achieve these membrane remodeling and lipid modifications and lipid enrichment is incompletely understood. Therefore, currently, there is a major ongoing effort to dissect the VRC assembly process and to understand the roles of viral and host factors in driving the biogenesis of VROs (1, 3, 7).

Tomato bushy stunt virus (TBSV), a plant-infecting tombusvirus, has been shown to induce complex rearrangements of cellular membranes and alterations in lipid and other metabolic processes during infections (8–10). The VROs formed during TBSV infections include extensive membrane contact sites (vMCSs) and harbor numerous spherules (containing VRCs), which are vesicle-like invaginations in the peroxisomal membranes (8, 11–13). A major gap in our understanding of the biogenesis of VROs, including vMCSs and VRCs, is how the cellular lipid-modifying enzymes are recruited to the sites of viral replication.

Tombusviruses belong to the large Flavivirus-like supergroup that includes important human, animal, and plant pathogens. Tombusviruses have a small single-component (+)RNA genome of ∼4.8 kb that codes for five proteins. Among those, there are two essential replication proteins, namely p33 and $p92^{pol}$, the latter of which is the RdRp protein and it is translated from the genomic RNA via readthrough of the translational stop codon in p33 open reading frame (14). The smaller p33 replication protein is an RNA chaperone, which mediates the selection of the viral (+)RNA for replication (14–16). Altogether, p33 is the master regulator of VRO biogenesis (3). We utilize a TBSV replicon (rep) RNA, which contains four noncontiguous segments from the genomic RNA, and it can efficiently replicate in yeast and plant cells expressing p33 and $p92^{pol}$ (14, 17).

Tombusviruses hijack various cellular compartments and pathways for VRO biogenesis (18). These include peroxisomes by TBSV or mitochondria (in the case of the closely related carnation Italian ringspot virus [CIRV]), the endoplasmic reticulum (ER) network, Rab1-positive COPII vesicles, and the Rab5-positive endosomes (8, 19–23). Tombusviruses also induce membrane

Significance

Replication of RNA viruses depends on the biogenesis of viral replication organelles (VROs). However, formation of VROs is not well understood. Using tombusviruses and the model host yeast, we discovered that the highly conserved host retromer complex is critical for the formation of VROs. Tombusvirus replication protein interacts with the retromer complex, leading to the recruitment of the retromer and its cargoes into VROs. The co-opted retromer tubular transport carriers deliver important enzymes required for lipid biosynthesis and lipid modifications that are needed for membrane biogenesis for efficient VRO assembly. Compartmentalization of these co-opted lipid enzymes within VROs gives a key advantage for tombusviruses to replicate in an optimized microenvironment and delay the antiviral responses of the hosts.

Author contributions: Z.F. and P.D.N. designed research; Z.F. and J.I. performed research; Z.F. and J.I. contributed new reagents/analytic tools; Z.F. and P.D.N. analyzed data; and Z.F. and P.D.N. wrote the paper.

The authors declare no competing interest.

This article is a PNAS Direct Submission.

[1]To whom correspondence may be addressed. Email: pdnagy2@uky.edu.

This article contains supporting information online at https://www.pnas.org/lookup/suppl/doi:10.1073/pnas.2016066118/-/DCSupplemental.

Published December 29, 2020.

proliferation, new lipid synthesis, and enrichment of lipids, most importantly phosphatidylethanolamine (PE), sterols, phosphatidylinositol-4-phosphate [PI(4)P], and phosphatidylinositol-3-phosphate [PI(3)P] phosphoinositides in peroxisomal or mitochondrial membranes for different tombusviruses (13, 24–27). This raised the question that how TBSV could hijack lipid synthesis enzymes from other subcellular locations that leads to enrichment of critical lipids in the large VROs in model yeast and plant hosts.

The endosomal network (i.e., early, late, and recycling endosomes) is a collection of pleomorphic organelles which sort membrane-bound proteins and lipids either for vacuolar/lysosomal degradation or recycling to other organelles. With the help of the so-called retromer complex, tubular transport carriers formed from the endosomes recycle cargoes to the Golgi and ER or to the plasma membrane (28–31). The core retromer complex consists of three conserved proteins, Vps26, Vps29, and Vps35, which are involved in cargo sorting and selection. The retromer complex affects several cellular processes, including autophagy through the maturation of lysosomes (32), neurodegenerative diseases (33), plant root hair growth (34), and plant immunity (35).

The cellular retromer is important for several pathogen–host interactions. For example, the retromer is targeted by *Brucella*, *Salmonella*, and *Legionella* bacteria (36–39) and the rice blast fungus (40). The retromer is also involved in the intracellular transport of the *Shigella* and *Cholera* toxins and the plant ricin toxin. The NS5A replication protein of hepatitis C virus (HCV) interacts with Vps35 and this interaction is important for HCV replication in human cells (41). The cytoplasmic tail of the Env protein of HIV-1 binds to the retromer components Vps35 and Vps26, which is required for Env trafficking and infectious HIV-1 morphogenesis (42). Moreover, the retromer complex affects the morphogenesis of vaccinia virus (43) and HPV16 human papillomavirus entry and delivery to the trans-Golgi network (44). Despite the importance of the retromer in pathogen–host interactions, the mechanistic insights are far from complete.

In the case of tombusviruses, enrichment of PE and PI(3)P within VROs is facilitated by co-opting the endosomal Rab5 small GTPase and Vps34 PI3K (20, 24), suggesting that the endosome-mediated trafficking pathway might be involved in viral replication in host cells. However, the actual mechanism of how tombusviruses exploit the endosomal/endocytic pathway and induce lipid enrichment within VROs is not yet dissected. Therefore, in this work, we targeted the retromer complex, based on previous genome-wide screens using yeast gene-deletion libraries, which led to the identification of *VPS29* and *VPS35* as host genes affecting TBSV replication and recombination, respectively (45, 46). These proteins are components of the retromer complex (28–31). We found TBSV and the closely related CIRV co-opt the retromer complex for the biogenesis of VROs in yeast and plants. We observed that depletion of retromer proteins strongly inhibited TBSV and CIRV replication. The recruitment of the retromer is driven by the viral p33 replication protein, which interacts with Vps26, Vps29, and Vps35 retromer proteins. We show that the retromer helps delivering critical cargo proteins, such as Psd2 phosphatidylserine decarboxylase, Vps34 phosphatidylinositol 3-kinase (PI3K), and Stt4 phosphatidylinositol 4-kinase (PI4Kα-like). These co-opted cellular enzymes are then involved in de novo production and enrichment of PE phospholipid, PI(3)P, and PI(4)P phosphoinositides within the VROs. Altogether, these virus-driven activities create an optimized membrane microenvironment within VROs to support efficient tombusvirus replication.

Results

Deletion of the Components of the Retromer Complex Inhibits Tombusvirus Replication in Yeast Cells. To characterize the putative role of the retromer complex in tombusvirus replication, we tested if TBSV replication in yeast cells depends on the Vps35p retromer component, which is a major cargo binding protein in the endosomes. TBSV replication was induced by expressing the p33 and $p92^{pol}$ replication proteins and the TBSV repRNA from plasmids in a vps35Δ yeast strain, followed by measuring TBSV repRNA accumulation by Northern blotting. These experiments showed that TBSV replication was reduced to a ∼20% level in the absence of Vps35p when compared to the replication level observed in the wild-type (WT) yeast (Fig. 1*A*, lanes 10–12 versus 1–3). We also observed the reduced accumulation of the viral p33 replication protein in vps35Δ yeast (Fig. 1*A*), suggesting decreased stability of p33. Complementation with a plasmid-borne WT Vps35p resulted in the recovery of tombusvirus replication to WT level in vps35Δ yeast (Fig. 1*A*, lanes 13–15). Interestingly, plasmid-borne expression of a Vps35p mutant ($R_{98}A/L_{99}P$), which is defective in the interaction with Vps26p (47), in vps35Δ yeast did not complement TBSV replication (Fig. 1*A*, lanes 16–18), suggesting that the formation of Vps35p–Vps26p complex is required for the proviral function of the retromer complex. Moreover, the expression of the Vps35 mutant ($R_{98}A/L_{99}P$) led to an approximately fourfold inhibition of TBSV repRNA accumulation in WT yeast (Fig. 1*A*, lanes 7–9 versus 1–3), likely due to the dominant-negative effect of the mutated Vps35p on the retromer functions. We also observed that the accumulation level of Vps35p was increased by 60% from its native promoter and original chromosomal location upon TBSV replication in WT yeast (Fig. 1*B*), suggesting that tombusvirus replication induces Vps35 messenger RNA (mRNA) expression in yeast.

To test if the closely related CIRV, which replicates on the outer membranes of mitochondria, also requires Vps35p, we compared CIRV replication in vps35Δ versus WT yeasts. The accumulation of repRNA in yeast decreased by approximately sevenfold in the absence of Vps35p (Fig. 1*C*, lanes 10–12), confirming the proviral function of Vps35 in CIRV replication. The accumulation level of p36, unlike that of $p95^{pol}$ replication protein, decreased in vps35Δ versus WT yeasts, suggesting reduced stability of the p36 replication protein in the absence of Vps35p (Fig. 1*C*). Expression of the plasmid-borne WT Vps35p in vps35Δ yeast increased repRNA accumulation by 50% in comparison with WT yeast (Fig. 1*C*, lanes 13–15). The $R_{98}A/L_{99}P$ mutant of Vps35p, which is defective in binding to Vps26, had a dominant-negative feature in viral replication when expressed in WT yeast (Fig. 1*C*, lanes 1–3). The $R_{98}A/L_{99}P$ mutant of Vps35p did not complement CIRV replication in vps35Δ yeast (Fig. 1*C*, lanes 16–18), confirming that the formation of the retromer complex is also needed for CIRV replication in yeast. Overall, we suggest that the retromer component Vps35p plays a critical proviral function both in the peroxisomal TBSV and the mitochondrial CIRV replication in yeast cells.

One function of Vps35p and the retromer could be the maintenance of the stability of TBSV p33 or CIRV p36 replication proteins in yeasts. To test if there is a direct proviral function of Vps35p, we used an in vitro TBSV replicase reconstitution assay, which included comparable amounts of purified recombinant p33 and $p92^{pol}$ replication proteins and yeast cell-free extracts (CFEs) (48) prepared from either WT or vps35Δ yeasts. The CFEs were programmed with the TBSV template repRNA. We found a ∼70% reduction in the newly made (+)repRNA progeny in CFEs prepared from vps35Δ yeast (Fig. 1*D*). The accumulation of the TBSV double-stranded RNA (dsRNA) replication intermediate, consisting of (−) and (+)RNAs (49), was also decreased by ∼50% (Fig. 1*D*), indicating that the Vps35p retromer component has a direct function supporting the assembly of the tombusvirus replicase complex in vitro.

To test if the other components of the retromer complex are also required for TBSV replication, we measured TBSV replication in vps26Δ and vps29Δ yeasts versus WT yeast. Deletion of these retromer genes resulted in an approximately four- to fivefold decrease in TBSV accumulation when compared with

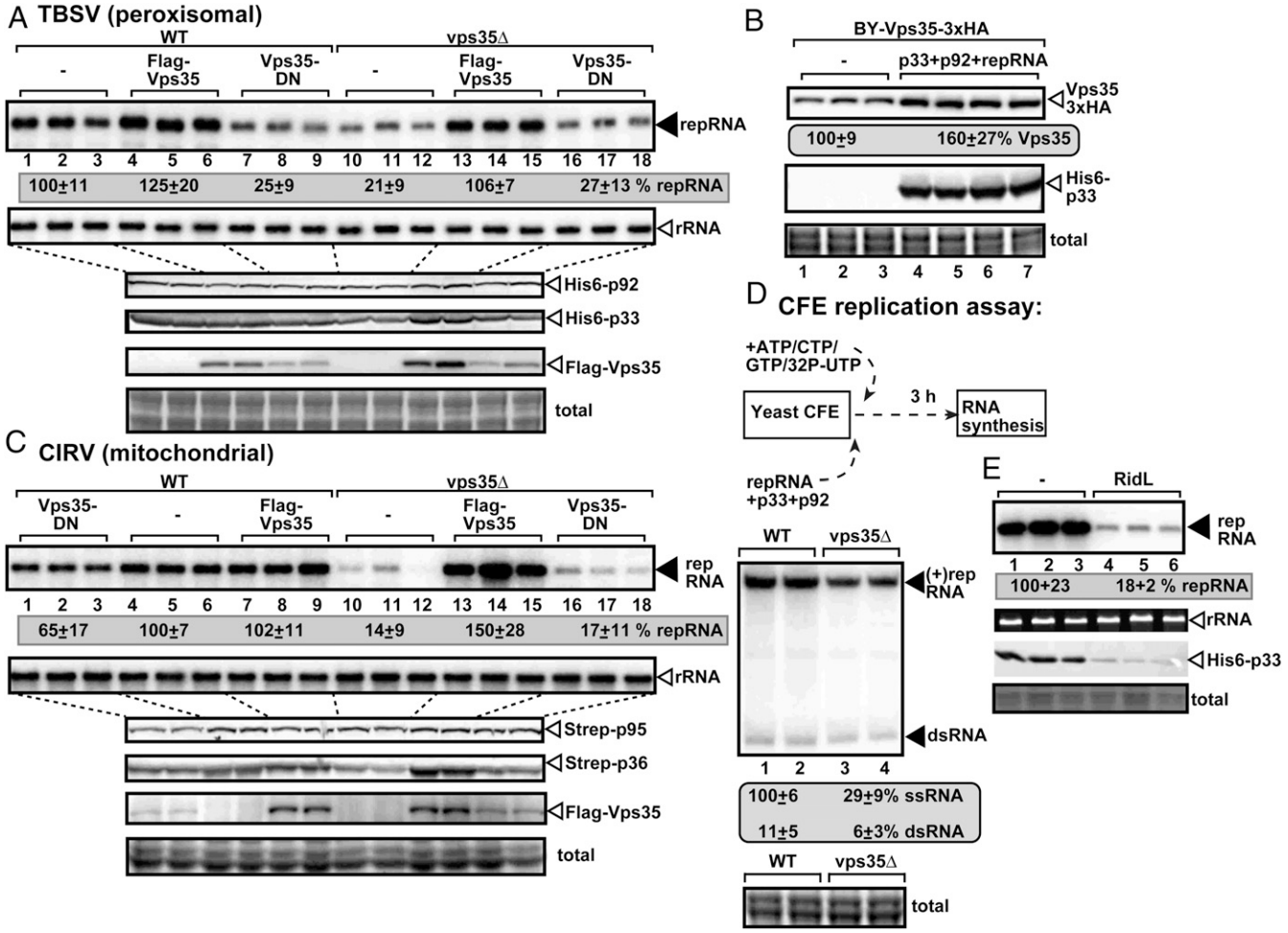

Fig. 1. Proviral role of the Vps35 retromer protein in tombusvirus replication in yeast. (*A*, *Top*) Northern blot analysis demonstrates decreased TBSV (+) repRNA accumulation in *vps35Δ* yeast strain. The viral replication proteins His_6-p33 and His_6-p92, together with the (+)repRNA were expressed from plasmids to support TBSV replication in yeast. Flag-tagged Vps35p and its dominant negative (DN) mutant were expressed from the constitutive *TEF1* promoter from a plasmid. The accumulation level of repRNA after 24-h replication was normalized based on 18S ribosomal RNA (rRNA) levels using Northern blotting (second panel). (*A*, *Bottom*) the accumulation of His_6-p33, His_6-p92, and Flag-Vps35 is measured by Western blotting and anti-His or anti-Flag antibodies. (*B*) Tombusvirus-induced expression of 3xHA-tagged Vps35p expressed from its natural chromosomal location and natural promoter in yeast after 24-h TBSV replication was detected by Western blotting with anti-HA antibody. (*C*) The replication of the mitochondrial membrane-associated CIRV in *vps35Δ* versus WT yeast strains was measured by Northern blotting. The p36 and p95 replication proteins of CIRV were tagged with a Strep tag and expressed from plasmids. See further details in *A*. (*D*) In vitro reconstitution of the TBSV replicase using purified recombinant MBP-p33 and MBP-$p92^{pol}$ and in vitro transcribed TBSV DI-72 (+)repRNA. The CFEs used for supporting the assembly of TBSV replicase complexes were prepared from the shown yeast strains. Nondenaturing polyacrylamide gel electrophoresis analysis shows the ^{32}P-labeled TBSV (+)repRNA progeny and the dsRNA replication intermediate, produced by the reconstituted replicase. The (+)repRNA progeny produced in WT CFE was chosen as 100. (*E*) The inhibitory effect of the *Legionella* RidL effector, which blocks retromer functions, on TBSV repRNA accumulation was measured by Northern blot 16 h after initiation of TBSV replication in *vps35Δ* versus WT (BY4741) yeast strains. The accumulation level of repRNA was normalized based on the rRNA. Second panel: ethidium bromide–stained gel with rRNA, as a loading control. Each experiment was performed three times.

WT yeast (*SI Appendix*, Fig. S1*A*, lanes 4–6 and 16–18 versus 10–12). Altogether, the level of reduction of TBSV replication was comparable in yeasts with deletion of each of the three retromer components (Fig. 1*A* and *SI Appendix*, Fig. S1*A*), suggesting that these retromer proteins likely work together as a complex to support TBSV replication in yeast. We were able to complement TBSV replication with plasmid-borne WT Vps26p and Vps29p in vps26Δ and vps29Δ yeasts, respectively, to validate the role of these proteins in TBSV replication (*SI Appendix*, Fig. S1*A*, lanes 1–3 and 19–21). Another similarity among vps35Δ, vps26Δ, and vps29Δ yeasts is the reduced accumulation of the TBSV p33 replication protein (Fig. 1*A* and *SI Appendix*, Fig. S1*A*), indicating a crucial role of the retromer complex in p33 stability in yeast. Similar findings were observed with the mitochondrial CIRV replication and stability of the p36 replication protein in vps26Δ and vps29Δ yeasts (*SI Appendix*, Fig. S1*B*). Therefore, all these data suggest that the whole retromer complex plays proviral functions during TBSV and CIRV replication in yeast.

To obtain additional evidence for the proviral function of the cellular retromer complex, we took advantage of the known antiretromer effect of a *Legionella* effector, namely RidL. *Legionella* secretes RidL to specifically bind to Vps29 and to block the retromer-based trafficking (39, 50). We expressed the full-length RidL in WT yeast replicating TBSV repRNA and showed an ~80% reduction in tombusvirus replication (Fig. 1*E*). As shown above with the retromer knockout mutants of yeast, the TBSV replication proteins accumulated to a reduced level in yeast expressing RidL (Fig. 1*E*). Therefore, we conclude that the cellular retromer complex plays a proviral role in tombusvirus replication.

The Cellular Retromer Complex Has Proviral Functions in Plants. To explore if tombusviruses depend on the retromer complex in plants, first we knocked down Vps35 expression based on tobacco rattle virus (TRV)-induced gene silencing (VIGS) in *Nicotiana benthamiana* plants (51, 52). Knockdown of Vps35 level in *N. benthamiana* resulted in an approximately sixfold reduction of the peroxisomal TBSV genomic (g)RNA and an approximately fourfold reduction in the mitochondrial CIRV RNA accumulation, respectively (Fig. 2 *A* and *C*, lanes 4–6). These findings demonstrated the proviral function of the plant Vps35 in tombusvirus replication. Knockdown of Vps35 delayed the symptom development and necrosis in systemic leaves infected with TBSV or CIRV (Fig. 2 *B* and *D*).

Comparable knockdown studies with the plant Vps26 and Vps29 retromer components via VIGS-based silencing in *N. benthamiana* plants revealed the dramatic reduction of TBSV and CIRV RNA accumulation (Fig. 2 *E* and *G*). An RT-PCR approach has confirmed the gene silencing of both Vps26 and Vps29 mRNAs in the corresponding *N. benthamiana* plants (Fig. 2*E*). The disease symptom formation and necrosis in systemic leaves caused by TBSV or CIRV infections were delayed upon knockdown of either Vps26 or Vps29 (Fig. 2 *F* and *H*).

Since viral RNA levels could also depend on viral cell-to-cell movement in whole plants, we also tested TBSV accumulation in the absence of virus spread using protoplasts (plant single cells lacking cell walls) isolated from Vps35-, Vps29-, and Vps26-silenced *N. benthamiana* plants, respectively. Comparable numbers of plant protoplasts were transfected with in vitro TBSV gRNA transcripts, followed by measuring TBSV RNA accumulation by Northern blotting 24 h later (Fig. 2*I*). The results showed ∼10% accumulation level of TBSV RNAs in protoplasts obtained from the retromer knockdown plants in comparison with the control plants (Fig. 2*I*). Based on the obtained data, we conclude that, similar to the results with the yeast host, the retromer complex acts as a crucial proviral factor in tombusvirus replication in plants.

We analyzed Vps35 mRNA levels in TBSV-infected or CIRV-infected versus mock-treated *N. benthamiana* leaves using RT-PCR. This revealed the up-regulation of Vps35 mRNA level in both TBSV-infected and CIRV-infected leaves (Fig. 2*J*). Thus, similar to yeast, tombusviruses can induce Vps35 mRNA expression in a plant host.

Tombusviruses Recruit the Retromer Complex into the VROs in Yeast and Plant Cells. To gain insights into the proviral function of the retromer complex, we tested the intracellular localization of the retromer components during tombusvirus replication. Confocal laser microscopy assays were performed after coexpressing blue fluorescent protein (BFP)-tagged p33 replication protein with green fluorescent protein (GFP)-tagged retromer components in *N. benthamiana* cells infected with TBSV. We found that Vps26, Vps29, and Vps35, respectively, were efficiently recruited into the large VROs marked by p33-BFP and the red fluorescent protein (RFP)-SKL peroxisomal marker protein (Fig. 3*A*). We observed a similar relocalization for the three retromer components, suggesting that they are co-opted as a complex into tombusvirus VROs. We extended this conclusion for CIRV infection, since the colocalization between the CIRV p36 replication protein and retromer components also supported the robust recruitment of the retromer complex into CIRV VROs (marked by CoxIV-RFP mitochondrial marker, Fig. 3*B*). On the contrary, coexpression of the retromer components with either RFP-SKL or CoxIV-RFP marker proteins did not show colocalization in plant cells in the absence of tombusvirus infections (*SI Appendix*, Fig. S2).

We also observed a similar relocalization pattern for the RFP-tagged Vps35p retromer component into the tombusviral VROs in yeast cells when either the GFP-tagged TBSV p33 or the CIRV GFP-p36 replication proteins were expressed in WT yeast cells (Fig. 3 *C* and *D*). The RFP-Vps35p localization pattern was different in the absence of viral components by showing small punctate distribution in yeast (*SI Appendix*, Fig. S2*C*). Based on these experiments, we conclude that the retromer complex is efficiently co-opted and retargeted by tombusvirus replication proteins into the large tombusvirus VROs in both plant and yeast cells.

Tombusvirus Replication Protein Interacts with Components of the Host Retromer Complex. To confirm that the host retromer complex is recruited into VROs through the interaction with the TBSV p33 replication proteins, we performed copurification experiments from yeast coexpressing Flag-Vps35p and TBSV His_6-p33 replication protein and replicating repRNA. The isolated membrane fraction of yeast cells was solubilized with a detergent and the Flag-Vps35p was affinity-purified, followed by Western blot analysis. We found that the His_6-p33 replication protein was efficiently copurified with Flag-Vps35p (Fig. 4*A*). In contrast, His_6-p33 was not detected in the control samples (Fig. 4*A*).

In the reciprocal copurification experiments, we expressed Vps35-3xHA from its natural promoter and the original chromosomal location in WT yeast. Then, the membrane fraction was solubilized and Flag-p33 was affinity-purified and detected by Western blotting. The purified Flag-p33 preparations contained Vps35-3xHA, confirming interaction between p33 and Vps35p in yeast membranes (Fig. 4*B*).

We performed similar copurification experiments using *N. benthamiana* plants. After coexpression of AtVps35-Flag with myc-tagged p33 replication protein in *N. benthamiana* leaves by agroinfiltration, and inoculation of the agroinfiltrated leaves with TBSV virions, we purified AtVps35-Flag from the detergent-solubilized membrane fraction. Western blotting resulted in detection of AtVps35-Flag and the copurified p33-myc replication protein via anti-myc antibody (Fig. 4*C*). Expression and purification of the Flag-tagged GFP was used as negative control (Fig. 4*C*).

To demonstrate if p33 could directly interact with the retromer components, we performed pull-down assays with purified recombinant MBP-tagged p33 replication protein and GST-tagged retromer components from *Escherichia coli*. We found that the MBP-p33 bound to amylose beads was able to capture the yeast Vps35, Vps26, and Vps29 retromer components and the plant AtVps35 (Fig. 4*D*). Thus, these data suggest direct interaction takes place between the tombusvirus p33 replication protein and the retromer components.

We also tested the interaction between AtVps29 and TBSV p33 replication protein via bimolecular fluorescence complementation (BiFC) in *N. benthamiana* plants infected with TBSV. Confocal images showed the interaction between AtVps29 and TBSV p33 occurred in VROs consisting of aggregated peroxisomes as visualized by RFP-SKL peroxisomal marker (Fig. 4*E* and *SI Appendix*, Fig. S3*B*). Similarly, the BiFC assay demonstrated the interaction between AtVps29 and CIRV p36, which occurred in VROs consisting of aggregated mitochondria (*SI Appendix*, Fig. S3). Altogether, our results confirmed the recruitment of the retromer complex into VROs both in yeast and plant cells.

The Co-Opted Retromer Facilitates the Recruitment of the Phosphatidylserine Decarboxylase (Psd2) Enzyme and Enrichment of PE Phospholipid within VROs. After providing evidence on the proviral roles of the retromer, we addressed the actual proviral functions of the retromer in TBSV replication. We have previously shown that TBSV induces the production and remarkable enrichment of PE within membranes of VROs (13). The PE enrichment depends on co-opting Rab5 GTPase-decorated endosomes, although the actual mechanism has not yet been revealed (20).

Based on the enrichment of PE within the tombusvirus VROs, we assumed that the TBSV-driven recruitment of the endosome-derived

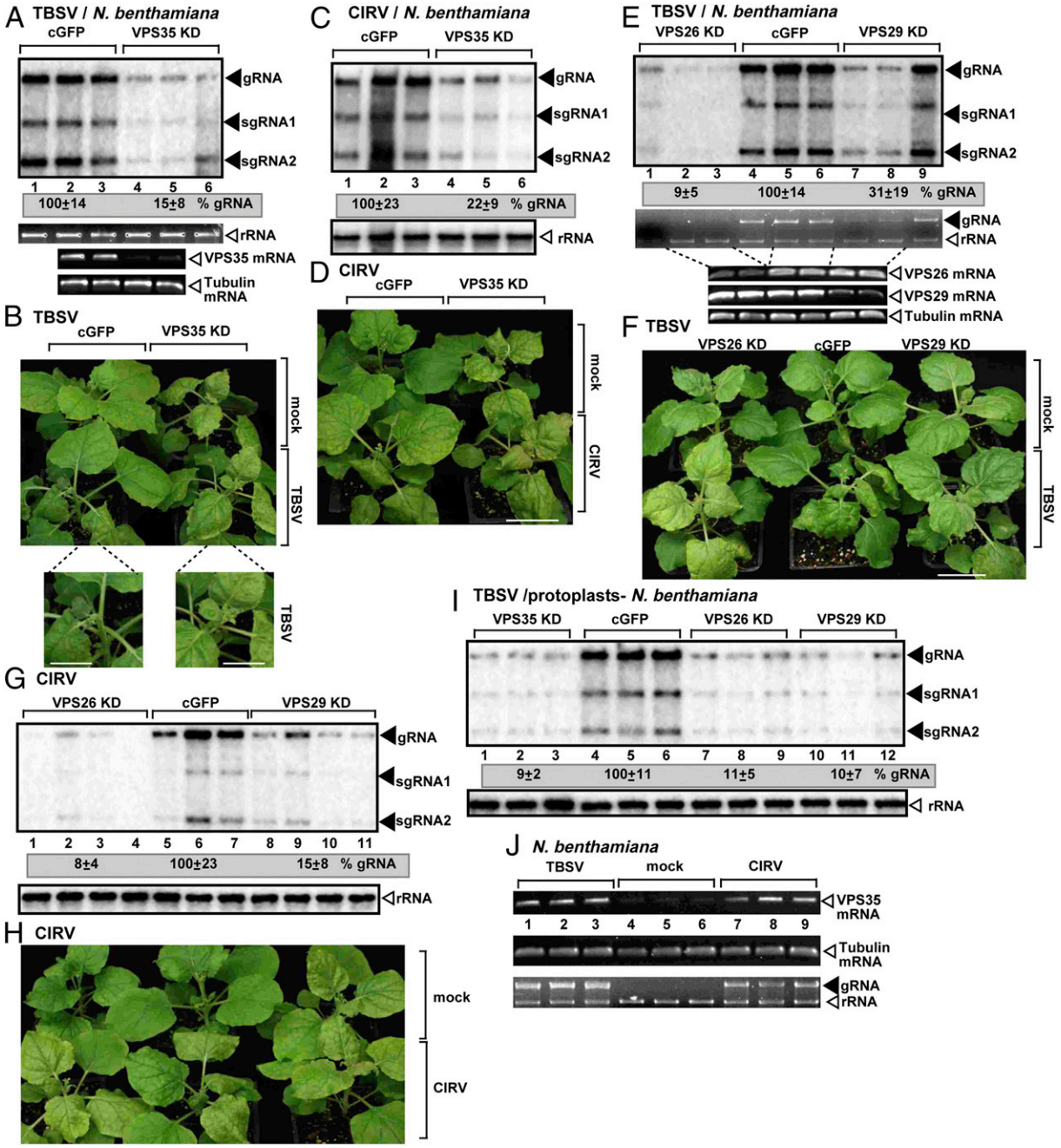

Fig. 2. Proviral roles of the retromer proteins in tombusvirus replication in plants. (*A*) VIGS-based knockdown of Vps35 mRNA level inhibits the accumulation of TBSV genomic RNA in *N. benthamiana*. (*Top*) The accumulation of TBSV gRNA and subgenomic RNAs (sgRNAs) was measured using Northern blot analysis of total RNA samples obtained from *N. benthamiana* leaves at 2 dpi. The systemically silenced upper leaves were inoculated with TBSV virions on the 12th day after VIGS. The control experiments included the TRV2-cGFP vector. Second panel: ethidium bromide–stained gel indicates ribosomal RNA level. (*Middle* and *Bottom*) The semiquantitative RT-PCR analyses of Vps35 mRNA and tubulin mRNA (control) levels, respectively, in the VIGS plants. (*B*) A moderate stunting phenotype is observed in Vps35 knockdown *N. benthamiana*. The enlarged images show the less severe symptoms caused by TBSV infection in the Vps35-silenced plants. The picture was taken 5 dpi. (Scale bars, 2 cm.) (*C*) VIGS-based knockdown of Vps35 inhibits the accumulation of CIRV genomic RNA in *N. benthamiana*. Samples for RNA extractions were taken 2.5 dpi from the inoculated leaves. See further details in *A*. (*D*) Ameliorating effect of Vps35 knockdown on symptoms caused by CIRV infection in *N. benthamiana*. (Scale bar, 5 cm.) (*E* and *G*) VIGS-based knockdown of Vps26 and Vps29 mRNA levels inhibit the accumulation of TBSV and CIRV gRNAs, respectively, in *N. benthamiana*. (*F* and *H*) Reduced symptom intensity in Vps26 and Vps29 knockdown plants caused by either TBSV or CIRV infections. See further details in *B*. (Scale bar, 5 cm.) (*I*) Northern blot analysis of TBSV gRNA accumulation in protoplasts obtained from the shown knockdown *N. benthamiana* plants. (*J*) Semiquantitative RT-PCR analyses of Vps35 mRNA and tubulin mRNA levels in TBSV or CIRV-infected versus mock-inoculated *N. benthamiana*. Samples for RNA extractions were taken 2.5 d after inoculation from the inoculated leaves.

retromer tubular transport carriers might be involved in PE enrichment within VROs. To test this hypothesis, we coexpressed RFP-tagged Psd2 phosphatidylserine decarboxylase, which produces PE from phosphatidylserine (PS), with GFP-p33 in WT and vps35Δ yeast strains replicating TBSV repRNA. Partial colocalization between p33 and Psd2p was visualized by confocal microscropy in WT yeast (Fig. 5*A*). In contrast, no significant overlap between p33 and Psd2p was captured in the vps35Δ yeast strain (Fig. 5*A*). Thus, these

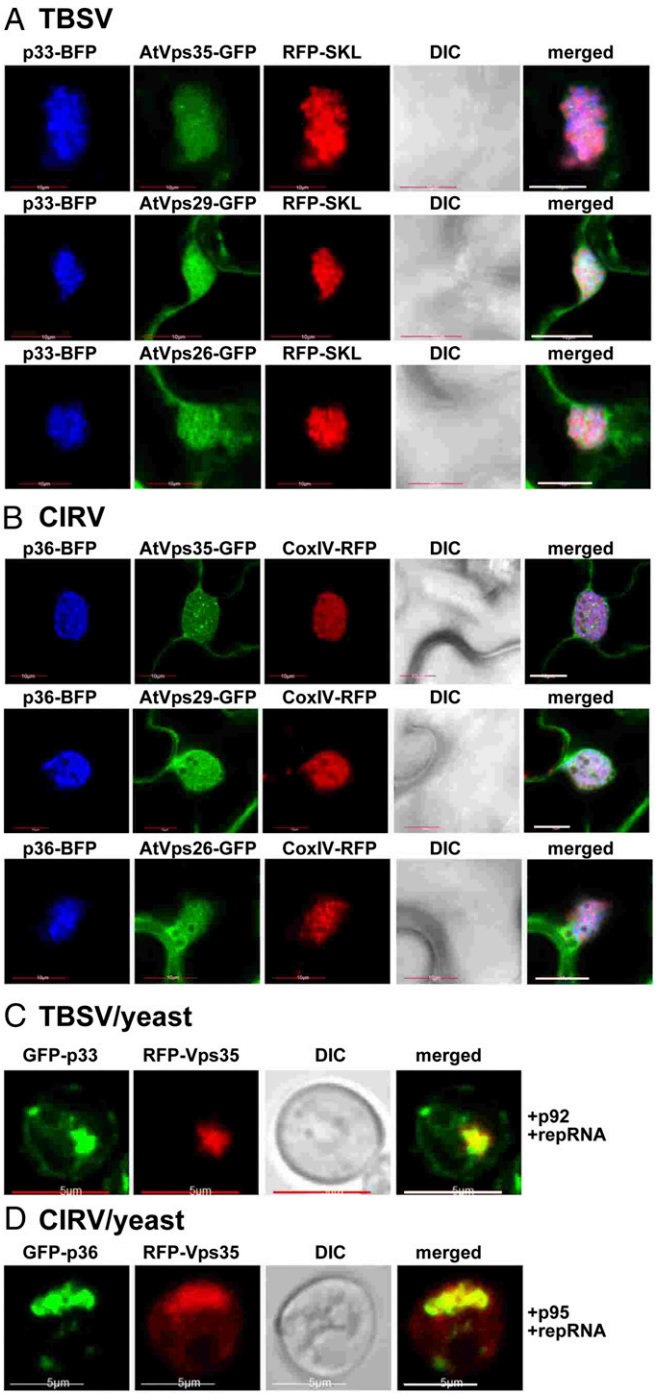

Fig. 3. Recruitment of the retromer proteins into VROs in plant cells infected with tombusviruses. (*A*) Colocalization of TBSV p33-BFP with the GFP-tagged Vps35, Vps29, and Vps26 proteins in *N. benthamiana* leaves infected with TBSV is detected by confocal microscopy. The VROs consisting of aggregated peroxisomes is marked with RFP-SKL peroxisomal luminar marker. (Scale bars, 10 μm.) (*B*) Colocalization of CIRV p36-BFP with the GFP-tagged Vps35, Vps29, and Vps26 proteins in *N. benthamiana* leaves infected with CIRV is detected by confocal microscopy. The VROs consisting of aggregated mitochondria are marked with CoxIV-RFP mitochondrial marker. (Scale bars, 10 μm.) (*C* and *D*) Recruitment of Vps35 into the VROs induced by either TBSV or CIRV replication proteins in WT yeast replicating TBSV repRNA. (Scale bars, 5 μm.) Each experiment was performed three times.

results imply that the retromer is involved in targeting of Psd2p phosphatidylserine decarboxylase into VROs, which in turn could contribute to local PE production in VROs.

To further determine the function of the retromer complex in PE enrichment within VROs, we tested PE distribution in yeast strains lacking one of the retromer components. Subcellular localization of PE is detected by using biotinylated duramycin peptide and streptavidin conjugated with Alexa Fluor 405. PE enrichment was not observed within VROs in vps35Δ, vps26Δ, or vps29Δ yeasts (Fig. 5*C*). In contrast, PE was highly enriched within VROs in WT yeast (Fig. 5*C*), as observed before (13).

To validate the yeast-based data in plants, we knocked down the Vps35 level in *N. benthamiana* plants, followed by protoplasts isolation. We observed the lack of PE enrichment within the p33-containing punctate structures (representing VROs) in Vps35 knockdown plant cells, suggesting that TBSV could not induce efficient PE enrichment in VROs when Vps35 retromer component was low in plant cells (Fig. 5*B*). In addition, we also observed that p33 did not induce the formation of the large aggregated structures in Vps35-silenced plant cells in comparison with the control plant cells. Collectively, these data support a central role for the retromer in Psd2 targeting and PE enrichment within the tombusviral VROs.

The Hijacked Retromer Transports Vps34 PI3K into the Tombusviral VROs for PI(3)P Enrichment. We have previously shown that TBSV co-opts the endosomal lipid kinase, Vps34 PI3K, which produces PI(3)P from PI phospholipid (24). This then leads to PI(3)P enrichment within VROs. The PI(3)P-enriched microenvironment is essential for optimal TBSV replication (24). However, the mode of recruitment of Vps34 PI3K into VROs is not known. Here, we have tested if the co-opted retromer-based tubular vesicles are involved in retargeting of Vps34 PI3K into VROs. Accordingly, we found that Vps34 PI3K was part of the hijacked retromer complex as shown via BiFC within VROs induced by TBSV or CIRV in *N. benthamiana* plants (Fig. 6 *A* and *B*).

To further understand the role of the retromer in Vps34 PI3K retargeting into VROs, we used deletion mutants of yeast retromer components. We observed the lack of efficient recruitment of Vps34p into VROs in vps35Δ, vps26Δ, or vps29Δ yeast strains (Fig. 6*C*). Therefore, the retromer is likely involved in the recruitment of the proviral Vps34 PI3K into VROs in yeast cells. Importantly, PI(3)P production and enrichment within VROs was not observed in vps35Δ, vps26Δ, or vps29Δ yeast strains (Fig. 6*D*). Immunofluorescence analysis with a PI3P antibody was also performed in plant protoplasts with a silenced Vps35 retromer component (Fig. 6*E*). Knocking down Vps35 level largely restricted PI(3)P enrichment within VROs detected via expression of p33-BFP. This conclusion is further supported by the intensity profile of additional images (*SI Appendix*, Fig. S4). Altogether, these findings imply that the co-opted retromer is required for delivering Vps34 PI3K to VROs and the local production and enrichment of PI(3)P within VROs, which are needed to support tombusvirus replication.

The Host PI4K Is Transported to the Tombusviral VROs for PI(4)P Production by the Co-Opted Retromer. Another important enzyme which might be co-opted with the help of the retromer tubular carriers is the yeast Stt4p PI4P kinase (PI4K) (53). PI4K has been shown to affect TBSV replication likely through providing PI(4)P for VRO assembly in yeast cells (27). PI(4)P is required for sterol and possibly PS enrichment within VROs. Accordingly, we observed the recruitment of Stt4p into VROs in WT yeast cells via confocal laser microscopy (Fig. 7*A*). On the contrary, Stt4p PI4K was not efficiently recruited into VROs in vps35Δ, vps26Δ, or vps29Δ yeast strains (Fig. 7*A*). Immunofluorescence analysis with a PI(4)P antibody was also performed in vps35Δ and vps29Δ yeast strains (Fig. 7*B*). Unlike in WT yeast,

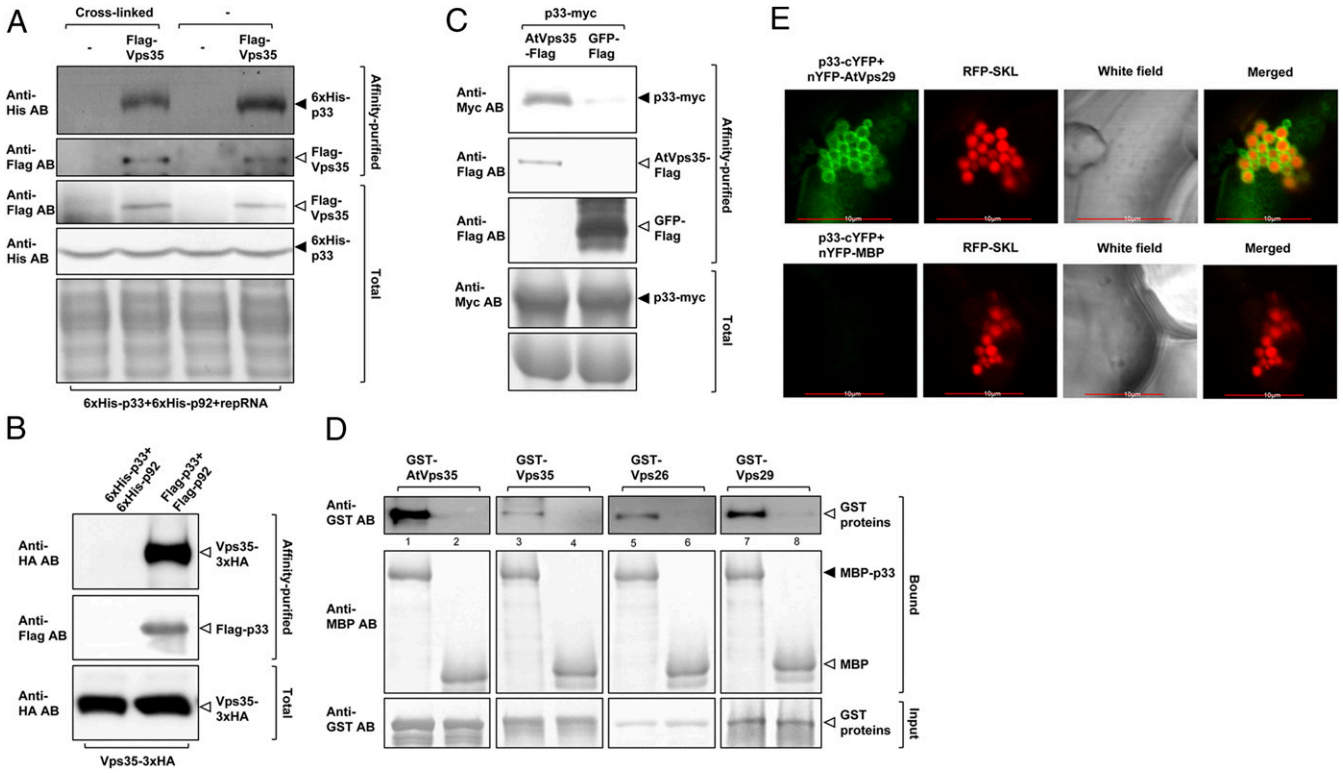

Fig. 4. Interaction between p33 replication protein and the retromer proteins. (*A*) Interaction between the yeast Vps35p and p33 replication protein in yeast based on copurification experiments. Top and second panels: Western blot analysis of purified Flag-tagged Vps35p and the copurified His_6-p33 from the solubilized membrane fraction of yeast. Flag-Vps35p and His_6-p33 were detected with anti-Flag and anti-His antibodies, respectively. The yeast samples were either cross-linked with formaldehyde or not cross-linked. Bottom panel: Western blots of Flag-Vps35 and His_6-p33 proteins in the total yeast extracts using anti-Flag and anti-His antibodies, respectively. (*B*) Copurification of the yeast Vps35-3xHA with the VRC. The viral replicase was affinity-purified via Flag column from solubilized membrane fraction of yeast. The yeast expressed Vps35-3xHA from the native promoter from the chromosome. See further details in *A*. (*C*) Copurification of the myc-tagged p33 replication protein with the Flag-tagged Vps35 from detergent-solubilized membrane fraction of *N. benthamiana* plant cells. The proteins were coexpressed from plasmids based on agroinfiltration of *N. benthamiana* leaves. The plants were also infected with TBSV. The bottom shows the Coomassie blue-stained polyacrylamide gel electrophoresis of the total protein extracts. (*D*) A pull-down assay to test direct binding between the MBP-p33 replication protein and the shown GST-tagged retromer proteins expressed in *E. coli*. The MBP-tagged p33 was immobilized on beads, followed by addition of the affinity-purified GST-tagged retromer proteins. MBP was used as a negative control. The bound or input proteins were detected via Western blot analysis with the shown antibodies. Each experiment was repeated three times. (*E*) BiFC assay to detect interaction between p33 replication protein and the Vps29 protein *in planta*. TBSV p33-cYFP and nYFP-Vps29 proteins were coexpressed from the 35S promoter after coagroinfiltration into *N. benthamiana* leaves. Note that the plants were infected with TBSV to induce VROs in cells. Colocalization of RFP-SKL with the BiFC signal indicates that the interaction between p33 and Vps29 proteins takes place within VROs. (Scale bars, 10 μm.)

the absence of either Vps35p or Vps29p retromer components prevented the enrichment of PI(4)P within VROs decorated by p33-BFP. These findings strongly indicate that the co-opted retromer is required for retargeting of the yeast Stt4p PI4P kinase into VROs, which in turn is needed for the de novo production and enrichment of PI(4)P within VROs in yeast cells.

Plants have the Stt4-like PI4Kα and the Pik1-like PI4Kβ with lipid kinase activity (54, 55). First, we have tested their mRNA levels upon infection of *N. benthamiana* plants with TBSV. qRT-PCR analysis showed ∼9- and ∼17-fold induction of PI4Kα and PI4Kβ mRNA levels, respectively, in TBSV-infected leaves (Fig. 7*C*). Subsequent work on PI4Kα with confocal microscopy demonstrated that PI4Kα was efficiently retargeted into the VROs induced by either TBSV or CIRV in *N. benthamiana* plants (Fig. 7*D*). Interestingly, knocking down Vps29 or Vps35 levels prevented the recruitment of PI4Kα into VROs induced by TBSV (Fig. 7*F*). Expression of the TBSV p33 replication protein alone induces VRO-like structure formation in *N. benthamiana* plants (*SI Appendix*, Fig. S5*A*). However, knocking down Vps35 levels prevented the recruitment of PI4Kα into the p33-induced VRO-like structure (*SI Appendix*, Fig. S5*A*). The overall level of GFP-PI4Kα within VROs is greatly diminished in Vps29 or Vps35 knockdown plants in comparison with the control plants (cGFP; Fig. 7*F* and *SI Appendix*, Fig. S5*A*). As expected based on the above data, colocalization experiments revealed the efficient retargeting of GFP-PI4Kα and Vps29-RFP into the p33-BFP–decorated VROs in plants infected with TBSV (*SI Appendix*, Fig. S5*B*).

Immunofluorescence analysis with a PI(4)P antibody confirmed that knocking down Vps35 retromer component in *N. benthamiana* protoplasts prevented the enrichment of PI(4)P within VROs decorated by p33-BFP (Fig. 7*E*). This is in contrast with the efficient enrichment of PI(4)P in the control *N. benthamiana* protoplasts (Fig. 7*E*). This conclusion is further supported by the intensity profile of additional images (*SI Appendix*, Fig. S6). Altogether, these findings strongly indicate that the co-opted retromer is required for retargeting of the PI4Kα kinase into VROs, which in turn is needed for the in situ production and enrichment of PI(4)P within VROs in plant cells.

To confirm that the co-opted PI4Ks have pro-TBSV functions in plants, we measured TBSV gRNA accumulation in PI4Kα- and PI4Kβ-silenced plants via Northern blotting. The dual silencing of PI4Kα and PI4Kβ resulted in 10-fold less accumulation of TBSV RNAs in *N. benthamiana* plants in comparison with the control plants (Fig. 7*G*). Note that individual silencing of PI4Kα led to

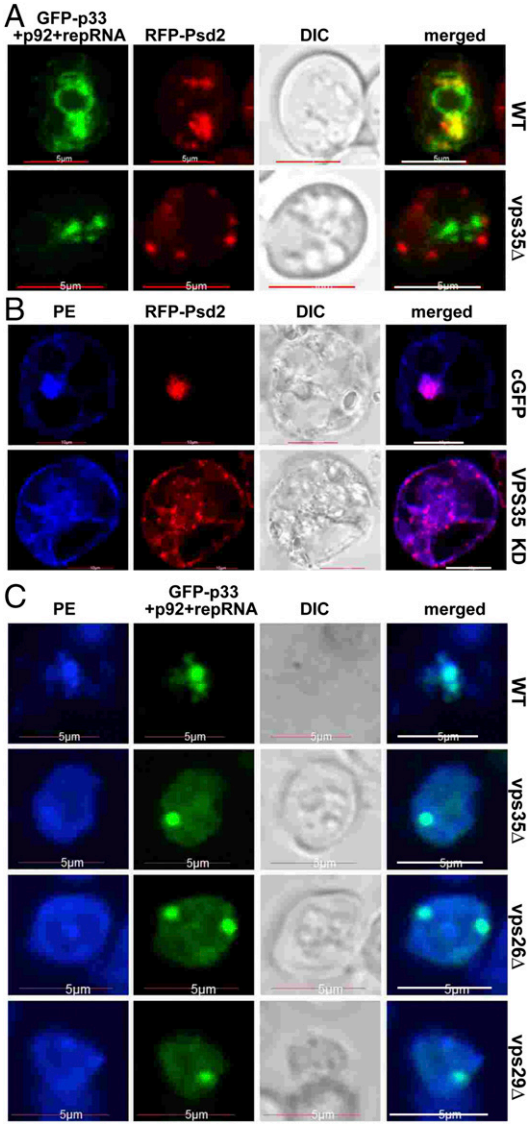

Fig. 5. Colocalization of TBSV p33 with Psd2 and enrichment of PE within VROs depend on the retromer in yeast and in *N. benthamiana*. (*A*) Confocal laser microscopy images show the lack of colocalization of TBSV GFP-p33 replication protein with the RFP-Psd2 protein in *vps35Δ* yeast versus their colocalization in WT yeast cells. DIC (differential interference contrast) images are shown. (Scale bars, 5 μm.) (*B*) VIGS-based knockdown of Vps35 level inhibits the enrichment of PE within TBSV VROs. The nonspecific VIGS control was a TRV vector carrying 3′ sequences of GFP (cGFP). Protoplasts were obtained from *N. benthamiana* leaves, followed by detection of PE distribution with biotinylated duramycin peptide and streptavidin conjugated with Alexa Fluor 405 and confocal microscopy. Each experiment was repeated three times. (Scale bars, 10 μm.) (*C*) Confocal laser microscopy images show the lack of PE enrichment and the lack of PE colocalization with the TBSV p33 replication protein in vps35Δ, vps26Δ, and vps29Δ yeasts. PE distribution was detected as described in *B*. (Scale bars, 5 μm.)

severe growth defects of *N. benthamiana* plants; therefore, we have not tested TBSV replication under this condition. Based on these results, we conclude that, with the assistance of the co-opted retromer, tombusviruses efficiently recruit PI4Ks into VROs in *N. benthamiana* plants to support local PI(4)P production.

Discussion

One of the emerging themes in RNA virus replication is that (+) RNA viruses rewire cellular pathways and extensively co-opt host proteins, intracellular membranes, and lipids to build large VROs, representing the sites of viral replication, inside the cytosol of the infected cells (5, 7, 10, 56–58). The membranous VROs also provide a protected subcellular environment for the viral RNAs, including the dsRNA replication intermediates against the host antiviral surveillance system (5, 6). A small number of viral replication proteins drives the formation of VROs by recruiting the host components (1, 59–65). However, the actual mechanism of building the VROs and remodeling of hijacked subcellular membranes by viruses is incompletely understood.

This major gap in knowledge is addressed with TBSV, which hijacks host components that lead to the biogenesis of large VROs consisting of aggregated peroxisomes and associated subdomains of the ER membranes (11, 19, 21). TBSV also exploits the endosomal network to enhance membrane surfaces for replication and induces phospholipid synthesis and modifies the lipid composition of VROs (13, 20, 24). However, it was not known how TBSV could accomplish these alterations in infected cells. In the current study, we have discovered that TBSV usurps the retromer complex and the tubular endosomal network to facilitate the delivery of a group of co-opted host factors, such as lipid enzymes, into tombusvirus VROs (Fig. 8). The retromer tubular transport carriers and their cargoes are likely needed to generate a protective microenvironment at the early replicase assembly/activation step. This is because we found that the synthesis of the TBSV dsRNA replication intermediate was inhibited in CFEs prepared from vps35Δ yeast. Whether the retromer components have additional direct roles in TBSV replication is currently not known.

The complete list of cellular proteins and lipids usurped by TBSV via hijacking the retromer and the tubular endosomal network is not yet fully defined. However, here we provide evidence that the retromer is needed for the delivery of three critical co-opted host factors to the VROs. Indeed, the lipid products of these hijacked cellular enzymes are key for the biogenesis of the TBSV VROs. First, we show that Psd2, which converts PS to PE, is co-opted into the VROs via the retromer. In the absence of TBSV, Psd2 is localized in the Golgi and vacuolar membranes (66, 67). The retargeting of Psd2 into the VROs may further facilitate the local production of PE, leading to PE enrichment needed for efficient TBSV replication. Indeed, depletion of retromer components inhibited PE enrichment within the VROs in both yeast and plant cells. The membranes of the tubular endosomal network are also likely used by TBSV and CIRV to increase the suitable membrane surfaces for viral replication within VROs. Overall, the highly PE-enriched membranes are crucial for virus replication in vitro in yeast and plant cells (13, 20).

Second, we show that the retromer facilitates the recruitment of Vps34 PI3K into the VROs. Vps34 produces PI(3)P phosphoinositide, which is an important signaling lipid in eukaryotic cells through interacting with many cellular proteins (68–70). PI(3)P is the signature lipid of the endosomal network in the cellular milieu. In the absence of the functional retromer, TBSV cannot enrich PI(3)P phosphoinositide within the VROs. We propose that the retromer-driven recruitment of Vps34 PI3K into the VROs facilitates in situ PI(3)P production. PI(3)P in turn likely facilitates additional recruitment of cellular enzymes into VROs.

The third lipid-modifying enzyme co-opted by TBSV with the help of the retromer tubular network is the yeast Stt4 PI4K and the plant PI4Kα. Stt4 and PI4Kα produce PI(4)P, which is needed by oxysterol binding proteins (OSBP in mammals) to exchange for sterols and allows the transfer of sterols and possibly PS phospholipid at the virus-induced membrane contact sites (vMCS) (27). The in situ productions of PI(3)P and PI(4)P minor structural lipids by the co-opted cellular PI3K and PI4K in the hijacked cellular membranes seem to be critical for proper VRO assembly and function. It is also possible that the local productions of PI(4)P and PI(3)P might allow tombusviruses to

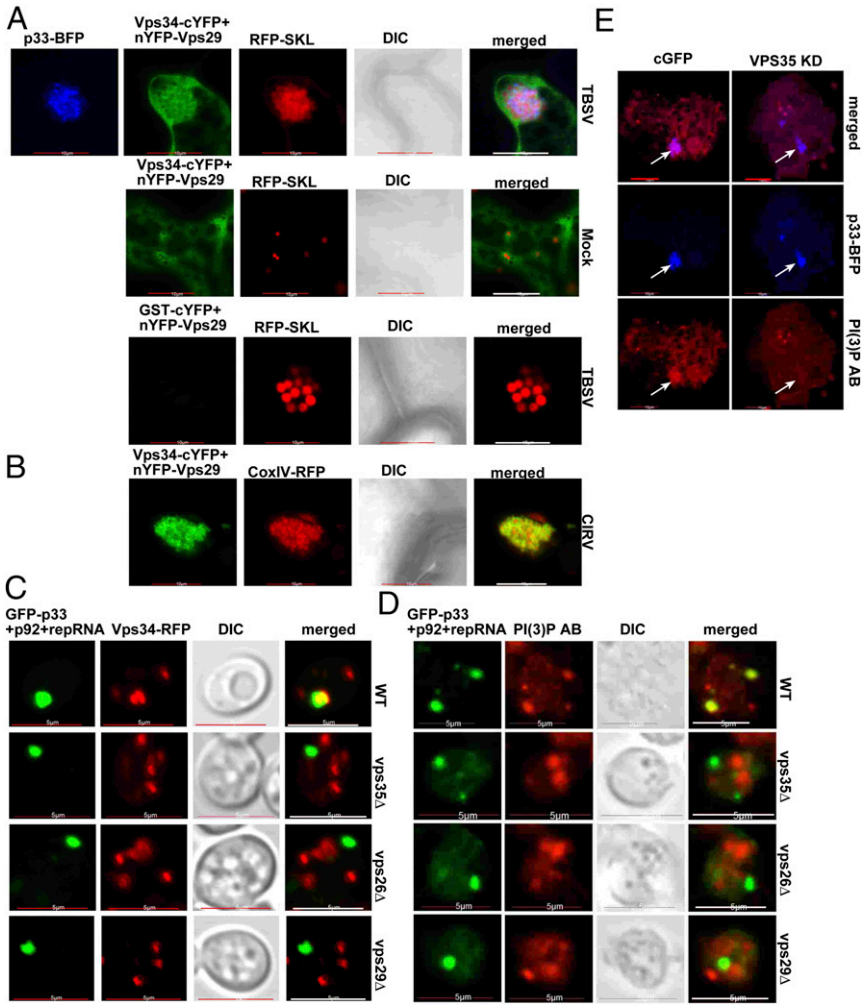

Fig. 6. Enrichment of PI(3)P phosphoinositide within VROs depends on the retromer proteins. (*A*) Interaction between Vps34 PI3K and Vps29 retromer protein within VROs is detected via BiFC in *N. benthamiana* infected with TBSV. The VROs were marked with p33-BFP and RFP-SKL expressed via agroinfiltration. Second panel: Vps34 PI3K interacts with Vps29 retromer protein in the absence of TBSV infection. However, the interaction does not take place in the peroxisomal membranes. (Scale bars, 10 μm.) (*B*) CIRV infection of *N. benthamiana* also results in the relocalization of Vps34 PI3K and Vps29 retromer protein into VROs. The CIRV VROs are marked with CoxIV-RFP, showing the characteristic aggregated mitochondria representing the site of CIRV replication. (Scale bars, 10 μm.) (*C*) The lack of recruitment of Vps34-RFP PI3K into VROs in vps35Δ, vps26Δ, and vps29Δ yeasts. The TBSV VROs were marked with GFP-p33. (Scale bars, 5 μm.) (*D*) The absence of local PI(3)P enrichment within VROs in vps35Δ, vps26Δ, and vps29Δ yeasts. PI(3)P was detected with anti-PI(3)P antibody. (Scale bars, 5 μm.) (*E*) VIGS-based knockdown of Vps35 inhibits the PI(3)P enrichment within TBSV VROs. The nonspecific VIGS control was a TRV-cGFP. Protoplasts were obtained from *N. benthamiana* leaves, followed by detection of PI(3)P distribution with anti-PI(3)P antibody and confocal microscopy. The TBSV VROs are marked with p33-BFP. (Scale bars, 10 μm.) Each experiment was repeated three times.

create membrane subdomains within the VROs that support different proviral functions (e.g., the formation of vMCSs versus VRC structures).

Altogether, we propose that TBSV hijacks the retromer complex-decorated tubular transport carriers in order to deliver the endosomal Psd2, Vps34 PI3K, and Stt4 PI4K and the PE-rich endosomal membranes into VROs for robust replication (Fig. 8). This co-opted function of the retromer is critical for the localized enrichment of PE phospholipid and PI(3)P and PI(4)P phosphoinositides within the VROs. The recruitment of the above endosomal enzymes to VROs likely facilitates the local de novo production of PI(3)P, PI(4)P, and PE from PS phospholipid. The in situ production and use of these critical lipids within subverted membranes likely allows tombusviruses to control spatially and temporally the replication and possibly the virion assembly steps within VROs. Moreover, co-opting enzymes required for lipid biosynthesis (i.e., PE) and lipid modifications [PI(3)P and PI(4)P] suggests that tombusviruses "force" the infected cells to create an optimal lipid/membrane microenvironment for efficient VRO assembly and protection of the viral RNAs during virus replication.

In summary, we have discovered that tombusviruses target a major crossroad in the secretory and recycling pathways via co-opting the retromer complex and the tubular endosomal network to build the large VROs in infected cells. Our findings of virus-mediated retargeting of the retromer complex should also be useful to understand the complex cellular functions of the retromer and identify potential cargoes of the tubular endosomal network and their roles in disease states. Altogether, by hijacking the retromer, tombusviruses co-opt cellular enzymes required for lipid biosynthesis and lipid modifications that facilitate optimal membranous milieu for VRO assembly. Based on these and previous findings, we propose that compartmentalization of these lipid enzymes within VROs gives a key advantage for

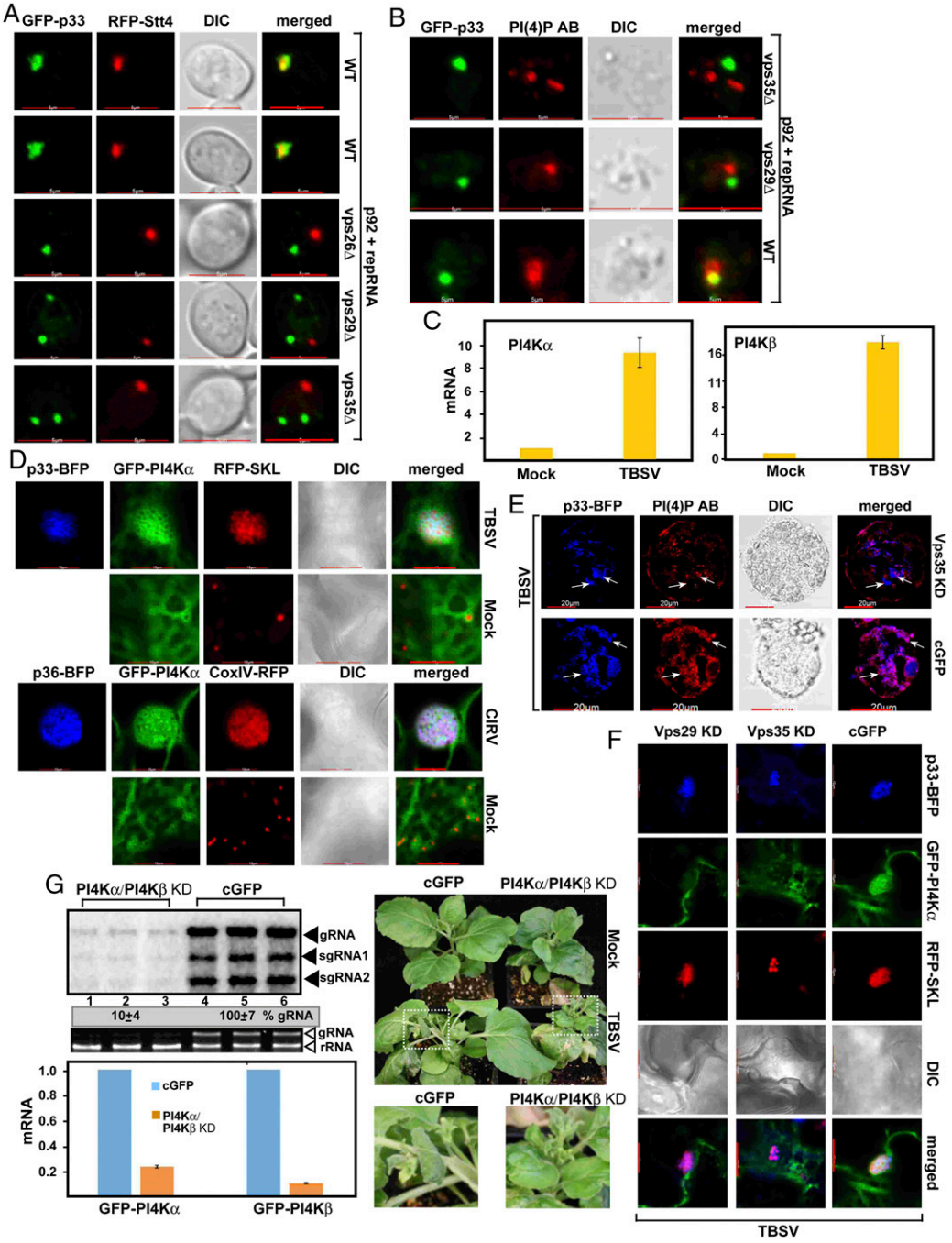

Fig. 7. Enrichment of PI(4)P phosphoinositide within VROs depends on the retromer proteins. (*A*) The lack of recruitment of RFP-Stt4p PI4K into VROs in vps35Δ, vps26Δ, and vps29Δ yeasts replicating TBSV repRNA. The TBSV VROs were marked with GFP-p33. (Scale bars, 5 μm.) (*B*) The absence of local PI(4)P enrichment within VROs in vps35Δ and vps29Δ yeasts, in contrast with the enrichment of PI(4)P within VROs in WT yeast. PI(4)P was detected with anti-PI(4)P antibody. (Scale bars, 5 μm.) (*C*) qRT-PCR analyses of PI4Kα1 and PI4Kβ1 mRNAs in TBSV-infected versus mock-inoculated *N. benthamiana*. Samples for RNA extractions were taken 5 d after inoculation from the systemic leaves. (*D*) Confocal images show the colocalization of either TBSV p33-BFP or CIRV p36-BFP replication proteins with the GFP-PI4Kα1 protein in *N. benthamiana* plants, which were infected or mock-inoculated. The TBSV VROs were marked with p33-BFP and RFP-SKL expressed via agroinfiltration, whereas CIRV VROs are marked with p36-BFP and CoxIV-RFP. DIC images are shown. (Scale bars, 10 μm.) (*E*) VIGS-based knockdown of Vps35 inhibits the enrichment of PI(4)P in TBSV VROs in *N. benthamiana* protoplasts. The TBSV VROs (pointed at by arrows) were marked with p33-BFP. (Scale bars, 20 μm.) (*F*) VIGS-based knockdown of Vps35 or Vps29 inhibits the retargeting of GFP-PI4Kα1 into TBSV VROs in *N. benthamiana* leaves. The nonspecific VIGS control was a TRV-cGFP. The TBSV VROs were marked with p33-BFP and RFP-SKL expressed via agroinfiltration and visualized via confocal microscopy. Note that plants were infected with TBSV. (*G*) VIGS-based knockdown of both PI4Kα1 and PI4Kβ1 mRNAs inhibits the accumulation of TBSV genomic RNA in *N. benthamiana*. (*Top Left*) The accumulation of TBSV gRNA was measured using Northern blot analysis of total RNA samples obtained from *N. benthamiana* leaves at 2 dpi. The leaves were inoculated with TBSV virions on the 10th day after VIGS. (*Middle Left*) Ethidium bromide–stained gel indicates ribosomal RNA level. *Right* also shows a moderate stunting phenotype is observed in PI4Kα1 and PI4Kβ1 knockdown *N. benthamiana*. The enlarged images (*Bottom Right*) show the less severe symptoms caused by TBSV infection in the PI4Kα1 and PI4Kβ1 silenced plants. The picture was taken 5 dpi. *Bottom Left* shows qRT-PCR analyses of PI4Kα1 and PI4Kβ1 mRNAs in the VIGS plants. Each experiment was performed three times.

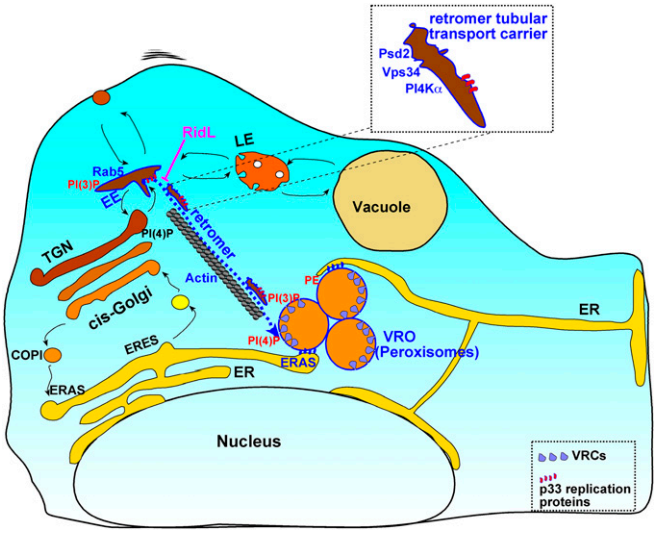

Fig. 8. A model of the role of the retromer tubular transport carriers in the biogenesis of tombusvirus VROs. We propose that the retromer-decorated tubular transport carriers help delivering critical cargoes, such as the Psd2 phosphatidylserine decarboxylase, Vps34, PI3K, and Stt4 PI4Kα-like into VROs, which represent the sites of viral replication. These co-opted cellular proteins are then involved in situ production and enrichment of PE phospholipid, PI(3)P, and PI(4)P phosphoinositides within the VROs. Altogether, these activities promote membrane-rich VRO biogenesis to support efficient tombusvirus replication. ERES, ER exit site for COP-II vesicles; ERAS, ER arrival site for COP-I vesicles; TGN, trans-Golgi network; EE, early endosome; LE, late endosome; RidL is a *Legionella* effector blocking retromer function. Membrane contact sites formed between part of the ER and VROs are shown with dark blue stripes.

tombusviruses to replicate in an efficient environment and avoid or delay the antiviral responses of the hosts.

Experimental Procedures

Yeast Strains. Parental yeast strain BY4741 (MATa his3Δ1 leu2Δ0 met15Δ0 ura3Δ0) and single-deletion strains vps35Δ, vps26Δ, and vps29Δ and were purchased from Open Biosystems. Yeast strain (BY4741: Vps35-3xHA) with chromosomal HA-tagged of *VPS35* was created by using yeast toolbox plasmids (71).

Plant and Yeast Expression Constructs. Plasmids and primers used in this study are provided in *SI Appendix*, Table S1.

Determination of Viral Replication in Yeast and Plant. To determine the function of the yeast retromer complex in the replication of TBSV and CIRV, yeast strains BY4741, vps35Δ, vps26Δ, and vps29Δ were transformed with plasmids pESC-His-p33/DI72, pYES-His-p92, and pRS315-cFlag or pRS315-Flag-Vps35 or pRS315-Vps26-Flag or pRS315-Vps29-Flag for TBSV replication and pESC-Strep-p36/DI72, pYES-Strep-p95, and pRS315-cFlag or pRS315-Flag-Vps35 or pRS315-Vps26-Flag or pRS315-Vps29-Flag for CIRV replication. The transformed yeast cells were pregrown in synthetic complete medium lacking uracil, leucine, and histidine (SC-ULH$^-$) supplemented with 2% glucose at 29 °C for overnight. Then, tombusvirus repRNA replication was induced in yeast by providing SC-ULH$^-$ supplemented with 2% galactose at 23 °C for 24 h for TBSV or 30 h for CIRV. Yeast total RNA and total protein were isolated and determined by Northern blotting and Western blotting, respectively (24).

To determine the effect of plant retromer complex on tombusvirus replication, NbVps35, NbVps26, or NbVps29 gene fragments were separately inserted into pTRV2 plasmid, and the corresponding gene expression was silenced using TRV-mediated VIGS approach in *N. benthamiana* (72). In each gene silencing experiment, the upper newly silenced leaves were inoculated with TBSV or CIRV sap 12 d after agroinfiltration. The TRV-cGFP control plants were treated in the same way. Plant leaf discs from inoculated leaves were sampled for viral RNA analysis by Northern blotting.

To determine the effect of plant PI4-kinases on tombusvirus replication, NbPI4Kα1 or NbPI4Kβ1 gene fragments were separately inserted into pTRV2 plasmid as above. Cosilencing of NbPI4Kα1 and NbPI4Kβ1 was performed by coagroinfiltration in a 1:1 ratio, and the upper newly silenced leaves were inoculated with TBSV sap 10 d after agroinfiltration.

Plant protoplasts were isolated from NbVps35 or NbVps26 or Vps29-silenced or cGFP-control *N. benthamiana* leaves (73). Equal amounts of protoplasts were used for each transformation. About 5×10^5 protoplasts were transfected with in vitro transcribed full-length TBSV genomic RNA, incubated in 35- × 10-mm Petri dishes in the dark at room temperature for 24 h. Total RNAs were isolated from these protoplasts, and viral RNAs level was determined by Northern blotting using [α-^{32}P]UTP radioactive-labeled RNA probes.

PE, PI(3)P and PI(4)P Enrichment within Viral Replication Compartments in Plant and Yeast. For PE enrichment analysis, plant protoplasts or yeast spheroplasts were isolated and immunofluorescence analysis was performed by using biotinylated duramycin peptide and streptavidin conjugated with Alexa Fluor 405 as described previously (13). For PI(3)P and PI(4)P enrichment analysis, plant protoplasts or yeast spheroplasts were isolated and immunofluorescence was performed by using either anti-PI(3)P or anti-PI(4)P antibody and secondary antibody conjugated with Alexa Fluor 568, as described previously (24, 27).

Additional materials and methods description can be found in *SI Appendix, Supplementary Material*.

Data Availability. All study data are included in the paper and *SI Appendix*.

ACKNOWLEDGMENTS. We thank Dr. Judit Pogany for critical reading of the manuscript and Dr. Kai Xu for providing RFP-Psd2 expression plasmid. This work was supported by the NSF (MCB-1122039 and IOS-1922895) and a US Department of Agriculture Hatch grant (KY012042) to P.D.N.

1. A. Wang, Dissecting the molecular network of virus-plant interactions: The complex roles of host factors. *Annu. Rev. Phytopathol.* **53**, 45–66 (2015).
2. I. Romero-Brey, R. Bartenschlager, Membranous replication factories induced by plus-strand RNA viruses. *Viruses* **6**, 2826–2857 (2014).
3. P. D. Nagy, Tombusvirus-host interactions: Co-opted evolutionarily conserved host factors take center court. *Annu. Rev. Virol.* **3**, 491–515 (2016).
4. T. X. Jordan, G. Randall, Flavivirus modulation of cellular metabolism. *Curr. Opin. Virol.* **19**, 7–10 (2016).
5. A. Shulla, G. Randall, (+) RNA virus replication compartments: A safe home for (most) viral replication. *Curr. Opin. Microbiol.* **32**, 82–88 (2016).
6. N. Kovalev, J. I. Inaba, Z. Li, P. D. Nagy, The role of co-opted ESCRT proteins and lipid factors in protection of tombusviral double-stranded RNA replication intermediate against reconstituted RNAi in yeast. *PLoS Pathog.* **13**, e1006520 (2017).
7. Z. Zhang *et al.*, Host lipids in positive-strand RNA virus genome replication. *Front. Microbiol.* **10**, 286 (2019).
8. I. Fernández de Castro, J. J. Fernández, D. Barajas, P. D. Nagy, C. Risco, Three-dimensional imaging of the intracellular assembly of a functional viral RNA replicase complex. *J. Cell Sci.* **130**, 260–268 (2017).
9. D. Barajas, I. F. Martín, J. Pogany, C. Risco, P. D. Nagy, Noncanonical role for the host Vps4 AAA+ ATPase ESCRT protein in the formation of Tomato bushy stunt virus replicase. *PLoS Pathog.* **10**, e1004087 (2014).
10. P. D. Nagy, J. Pogany, The dependence of viral RNA replication on co-opted host factors. *Nat. Rev. Microbiol.* **10**, 137–149 (2011).
11. D. Barajas *et al.*, Co-opted oxysterol-binding ORP and VAP proteins channel sterols to RNA virus replication sites via membrane contact sites. *PLoS Pathog.* **10**, e1004388 (2014).
12. K. Xu, P. D. Nagy, Sterol binding by the tombusviral replication proteins is essential for replication in yeast and plants. *J. Virol.* **91**, e01984-16 (2017).
13. K. Xu, P. D. Nagy, RNA virus replication depends on enrichment of phosphatidylethanolamine at replication sites in subcellular membranes. *Proc. Natl. Acad. Sci. U.S.A.* **112**, E1782–E1791 (2015).
14. K. A. White, P. D. Nagy, Advances in the molecular biology of tombusviruses: Gene expression, genome replication, and recombination. *Prog. Nucleic Acid Res. Mol. Biol.* **78**, 187–226 (2004).
15. J. Stork, N. Kovalev, Z. Sasvari, P. D. Nagy, RNA chaperone activity of the tombusviral p33 replication protein facilitates initiation of RNA synthesis by the viral RdRp in vitro. *Virology* **409**, 338–347 (2011).
16. J. Pogany, K. A. White, P. D. Nagy, Specific binding of tombusvirus replication protein p33 to an internal replication element in the viral RNA is essential for replication. *J. Virol.* **79**, 4859–4869 (2005).
17. T. Panavas, P. D. Nagy, Yeast as a model host to study replication and recombination of defective interfering RNA of Tomato bushy stunt virus. *Virology* **314**, 315–325 (2003).

18. P. D. Nagy, J. Pogany, K. Xu, Cell-free and cell-based approaches to explore the roles of host membranes and lipids in the formation of viral replication compartment induced by tombusviruses. *Viruses* **8**, 68 (2016).
19. Z. Sasvari, N. Kovalev, P. A. Gonzalez, K. Xu, P. D. Nagy, Assembly-hub function of ER-localized SNARE proteins in biogenesis of tombusvirus replication compartment. *PLoS Pathog.* **14**, e1007028 (2018).
20. K. Xu, P. D. Nagy, Enrichment of phosphatidylethanolamine in viral replication compartments via Co-opting the endosomal Rab5 small GTPase by a positive-strand RNA virus. *PLoS Biol.* **14**, e2000128 (2016).
21. K. B. Pathak, Z. Sasvari, P. D. Nagy, The host Pex19p plays a role in peroxisomal localization of tombusvirus replication proteins. *Virology* **379**, 294–305 (2008).
22. M. Jonczyk, K. B. Pathak, M. Sharma, P. D. Nagy, Exploiting alternative subcellular location for replication: Tombusvirus replication switches to the endoplasmic reticulum in the absence of peroxisomes. *Virology* **362**, 320–330 (2007).
23. J. I. Inaba *et al*., Screening *Legionella* effectors for antiviral effects reveals Rab1 GTPase as a proviral factor coopted for tombusvirus replication. *Proc. Natl. Acad. Sci. U.S.A.* **116**, 21739–21747 (2019).
24. Z. Feng, K. Xu, N. Kovalev, P. D. Nagy, Recruitment of Vps34 PI3K and enrichment of PI3P phosphoinositide in the viral replication compartment is crucial for replication of a positive-strand RNA virus. *PLoS Pathog.* **15**, e1007530 (2019).
25. M. Sharma, Z. Sasvari, P. D. Nagy, Inhibition of phospholipid biosynthesis decreases the activity of the tombusvirus replicase and alters the subcellular localization of replication proteins. *Virology* **415**, 141–152 (2011).
26. M. Sharma, Z. Sasvari, P. D. Nagy, Inhibition of sterol biosynthesis reduces tombusvirus replication in yeast and plants. *J. Virol.* **84**, 2270–2281 (2010).
27. Z. Sasvari *et al*., Co-opted cellular Sac1 lipid phosphatase and PI(4)P phosphoinositide are key host factors during the biogenesis of the tombusvirus replication compartment. *J. Virol.* **94**, e01979-19 (2020).
28. B. Simonetti, P. J. Cullen, Endosomal sorting: Architecture of the retromer coat. *Curr. Biol.* **28**, R1350–R1352 (2018).
29. O. Kovtun *et al*., Structure of the membrane-assembled retromer coat determined by cryo-electron tomography. *Nature* **561**, 561–564 (2018).
30. L. Johannes, C. Wunder, Retromer sets a trap for endosomal cargo sorting. *Cell* **167**, 1452–1454 (2016).
31. C. Burd, P. J. Cullen, Retromer: A master conductor of endosome sorting. *Cold Spring Harb. Perspect. Biol.* **6**, a016774 (2014).
32. Y. Cui *et al*., Retromer has a selective function in cargo sorting via endosome transport carriers. *J. Cell Biol.* **218**, 615–631 (2019).
33. C. Reitz, Retromer dysfunction and neurodegenerative disease. *Curr. Genomics* **19**, 279–288 (2018).
34. S. G. Jha *et al*., Vacuolar Protein Sorting 26C encodes an evolutionarily conserved large retromer subunit in eukaryotes that is important for root hair growth in Arabidopsis thaliana. *Plant J.* **94**, 595–611 (2018).
35. D. Munch *et al*., Retromer contributes to immunity-associated cell death in Arabidopsis. *Plant Cell* **27**, 463–479 (2015).
36. K. L. Patrick *et al*., Quantitative yeast genetic interaction profiling of bacterial effector proteins uncovers a role for the human retromer in Salmonella infection. *Cell Syst.* **7**, 323–338.e6 (2018).
37. V. Singh *et al*., Cholera toxin inhibits SNX27-retromer-mediated delivery of cargo proteins to the plasma membrane. *J. Cell Sci.* **131**, jcs218610 (2018).
38. A. Casanova *et al*., A role for the VPS retromer in *Brucella* intracellular replication revealed by genomewide siRNA screening. *mSphere* **4**, e00380-19 (2019).
39. K. Bärlocher *et al*., Structural insights into Legionella RidL-Vps29 retromer subunit interaction reveal displacement of the regulator TBC1D5. *Nat. Commun.* **8**, 1543 (2017).
40. W. Zheng *et al*., Retromer is essential for autophagy-dependent plant infection by the rice blast fungus. *PLoS Genet.* **11**, e1005704 (2015).
41. P. Yin, Z. Hong, X. Yang, R. T. Chung, L. Zhang, A role for retromer in hepatitis C virus replication. *Cell. Mol. Life Sci.* **73**, 869–881 (2016).
42. E. Groppelli, A. C. Len, L. A. Granger, C. Jolly, Retromer regulates HIV-1 envelope glycoprotein trafficking and incorporation into virions. *PLoS Pathog.* **10**, e1004518 (2014).
43. K. Harrison *et al*., Vaccinia virus uses retromer-independent cellular retrograde transport pathways to facilitate the wrapping of intracellular mature virions during virus morphogenesis. *J. Virol.* **90**, 10120–10132 (2016).
44. A. Popa *et al*., Direct binding of retromer to human papillomavirus type 16 minor capsid protein L2 mediates endosome exit during viral infection. *PLoS Pathog.* **11**, e1004699 (2015).
45. E. Serviene *et al*., Genome-wide screen identifies host genes affecting viral RNA recombination. *Proc. Natl. Acad. Sci. U.S.A.* **102**, 10545–10550 (2005).
46. T. Panavas, E. Serviene, J. Brasher, P. D. Nagy, Yeast genome-wide screen reveals dissimilar sets of host genes affecting replication of RNA viruses. *Proc. Natl. Acad. Sci. U.S.A.* **102**, 7326–7331 (2005).
47. S. Gokool, D. Tattersall, J. V. Reddy, M. N. Seaman, Identification of a conserved motif required for Vps35p/Vps26p interaction and assembly of the retromer complex. *Biochem. J.* **408**, 287–295 (2007).
48. J. Pogany, J. Stork, Z. Li, P. D. Nagy, In vitro assembly of the Tomato bushy stunt virus replicase requires the host Heat shock protein 70. *Proc. Natl. Acad. Sci. U.S.A.* **105**, 19956–19961 (2008).
49. N. Kovalev, J. Pogany, P. D. Nagy, Template role of double-stranded RNA in tombusvirus replication. *J. Virol.* **88**, 5638–5651 (2014).
50. J. Yao *et al*., Mechanism of inhibition of retromer transport by the bacterial effector RidL. *Proc. Natl. Acad. Sci. U.S.A.* **115**, E1446–E1454 (2018).
51. S. Schellmann, P. Pimpl, Coats of endosomal protein sorting: Retromer and ESCRT. *Curr. Opin. Plant Biol.* **12**, 670–676 (2009).
52. S. P. Dinesh-Kumar, R. Anandalakshmi, R. Marathe, M. Schiff, Y. Liu, Virus-induced gene silencing. *Methods Mol. Biol.* **236**, 287–294 (2003).
53. A. Audhya, M. Foti, S. D. Emr, Distinct roles for the yeast phosphatidylinositol 4-kinases, Stt4p and Pik1p, in secretion, cell growth, and organelle membrane dynamics. *Mol. Biol. Cell* **11**, 2673–2689 (2000).
54. H. W. Xue, C. Pical, C. Brearley, S. Elge, B. Müller-Röber, A plant 126-kDa phosphatidylinositol 4-kinase with a novel repeat structure. Cloning and functional expression in baculovirus-infected insect cells. *J. Biol. Chem.* **274**, 5738–5745 (1999).
55. J. M. Stevenson, I. Y. Perera, W. F. Boss, A phosphatidylinositol 4-kinase pleckstrin homology domain that binds phosphatidylinositol 4-monophosphate. *J. Biol. Chem.* **273**, 22761–22767 (1998).
56. I. F. de Castro, L. Volonté, C. Risco, Virus factories: Biogenesis and structural design. *Cell. Microbiol.* **15**, 24–34 (2013).
57. G. A. Belov, F. J. van Kuppeveld, (+)RNA viruses rewire cellular pathways to build replication organelles. *Curr. Opin. Virol.* **2**, 740–747 (2012).
58. J. A. den Boon, P. Ahlquist, Organelle-like membrane compartmentalization of positive-strand RNA virus replication factories. *Annu. Rev. Microbiol.* **64**, 241–256 (2010).
59. S. Reiss *et al*., Recruitment and activation of a lipid kinase by hepatitis C virus NS5A is essential for integrity of the membranous replication compartment. *Cell Host Microbe* **9**, 32–45 (2011).
60. K. A. Stapleford, D. J. Miller, Role of cellular lipids in positive-sense RNA virus replication complex assembly and function. *Viruses* **2**, 1055–1068 (2010).
61. K. Xu, P. D. Nagy, Expanding use of multi-origin subcellular membranes by positive-strand RNA viruses during replication. *Curr. Opin. Virol.* **9**, 119–126 (2014).
62. N. Altan-Bonnet, Lipid tales of viral replication and transmission. *Trends Cell Biol.* **27**, 201–213 (2017).
63. H. M. van der Schaar, C. M. Dorobantu, L. Albulescu, J. R. P. M. Strating, F. J. M. van Kuppeveld, Fat(al) attraction: Picornaviruses usurp lipid transfer at membrane contact sites to create replication organelles. *Trends Microbiol.* **24**, 535–546 (2016).
64. I. Fernández de Castro, R. Tenorio, C. Risco, Virus assembly factories in a lipid world. *Curr. Opin. Virol.* **18**, 20–26 (2016).
65. C. Harak, V. Lohmann, Ultrastructure of the replication sites of positive-strand RNA viruses. *Virology* **479-480**, 418–433 (2015).
66. D. R. Voelker, Phosphatidylserine decarboxylase. *Biochim. Biophys. Acta* **1348**, 236–244 (1997).
67. K. Muthukumar, V. Nachiappan, Phosphatidylethanolamine from phosphatidylserine decarboxylase2 is essential for autophagy under cadmium stress in Saccharomyces cerevisiae. *Cell Biochem. Biophys.* **67**, 1353–1363 (2013).
68. S. D. Kale *et al*., External lipid PI3P mediates entry of eukaryotic pathogen effectors into plant and animal host cells. *Cell* **142**, 284–295 (2010).
69. V. Deretic *et al*., Mycobacterium tuberculosis inhibition of phagolysosome biogenesis and autophagy as a host defence mechanism. *Cell. Microbiol.* **8**, 719–727 (2006).
70. F. A. Horenkamp *et al*., The Legionella anti-autophagy effector RavZ targets the autophagosome via PI3P- and curvature-sensing motifs. *Dev. Cell* **34**, 569–576 (2015).
71. C. Janke *et al*., A versatile toolbox for PCR-based tagging of yeast genes: New fluorescent proteins, more markers and promoter substitution cassettes. *Yeast* **21**, 947–962 (2004).
72. S. Bachan, S. P. Dinesh-Kumar, Tobacco rattle virus (TRV)-based virus-induced gene silencing. *Methods Mol. Biol.* **894**, 83–92 (2012).
73. S. D. Yoo, Y. H. Cho, J. Sheen, Arabidopsis mesophyll protoplasts: A versatile cell system for transient gene expression analysis. *Nat. Protoc.* **2**, 1565–1572 (2007).